JOURNAL OF MAGNETIC RESONANCE **133,** 255–265 (1998)
ARTICLE NO. MN981465

Vicinal Fluorine–Proton Coupling Constants

II. Individual Substituent Effects

J. San Fabián,[1] J. Guilleme, and E. Díez

Facultad de Ciencias, C-2, Universidad Autónoma de Madrid, 28049-Madrid, Spain

Received November 6, 1997; revised March 18, 1998

The angular dependence and the effect of individual substituents upon the NMR vicinal fluorine–proton couplings $^3J_{FH}$ have been studied using data sets of experimental and calculated couplings. Coupling constants for a series of fluoroethane derivatives, $CHXF–CH_3$ and $CH_2F–CH_2X$ ($X = CH_3$, NH_2, OH, and F), were calculated by means of the SCF *ab initio* and semiempirical INDO/FPT methods. The calculated couplings reproduce correctly the main experimental trends in spite of the limitation in the calculation because of lack of electronic correlation and the use of medium size basis set. The individual substituent effects $\Delta K_{ni}^{X_i}$ are described by quadratic expressions on the relative electronegativities of substituents $\Delta\chi_{X_i}$ ($\Delta K_{ni}^{X_i} = k_{ni}^0 + k_{ni}\Delta\chi_{X_i} + k_{nii}\Delta\chi_{X_i}^2$). A selected data set of 58 experimental couplings, ranging from 1.9 to 44.4 Hz, has been collected from the literature. An extended Karplus equation with 16 coefficients that includes the electronegativity substituent effects has been derived from the experimental data set with a root-mean-square deviation of 1.2 Hz.

Key Words: **NMR spin coupling; vicinal F–H coupling constants; SCF *ab initio* calculations; individual substituent effects; extended Karplus equation; empirical parameterization.**

INTRODUCTION

The NMR vicinal coupling constants are a powerful tool for structural elucidation and conformational analysis of molecules in solution (*1, 2*). The reliability of the information about the conformational behavior of molecules obtained from the vicinal couplings depends largely on the accuracy of the available equations relating the value of these couplings with the molecular geometry. Relatively complex equations have been derived for the proton–proton vicinal coupling constants $^3J_{HH}$ which predict the coupling values with an uncertainty close to 0.4 Hz (*3–10*). Less accurate equations have been derived for other vicinal couplings: carbon–proton, proton–nitrogen, carbon–carbon, etc. (see (*1*) and references cited therein). The equations for these couplings do not include, in general, the substituent effects in an explicit way, and their parameterization, for specific groups of molecules, is based on the well-known Karplus equation (*11, 12*). On the other hand, and in spite of the increasing importance of the fluoro-compounds in pharmacological areas (*13*), the F–H and F–F vicinal couplings still have a relatively small importance in conformational analysis owing, in part, to the difficulty in treating the substituent effects (*14*). The aim of this series of studies is to overcome this difficulty by analyzing a set of $^3J_{FH}$ couplings calculated by *ab initio* methods in a framework of models and equations for the substituent effects.

A Karplus-type dependence for the vicinal fluorine–proton couplings was confirmed empirically by Williamson *et al.* (*15, 16*) and theoretically by Govil (*17*) and Gophinathan *et al.* (*18*). The substituent effects upon $^3J_{FH}$ couplings were also studied during the 1960s and 1970s (*17, 19–24*). However, while the empirical results showed a rough linear (*19, 20*) or exponential (*23, 25*) decay of $^3J_{FH}$ as the electronegativity of the substituents increases, the theoretical calculations, which were done with semiempirical methods, predicted, in some situations, the opposite behavior (*17*).

The vicinal coupling constants depend on several factors: torsional angles ϕ between the coupled nuclei, nature and position of substituents, changes in bond lengths and bond angles, etc. The range of the $^3J_{FH}$ couplings is about three times larger than that of the proton–proton couplings. Consequently, the effects of the different factors on $^3J_{FH}$ are, in general, increased proportionally. Therefore, these effects may be detected and analyzed more easily for the $^3J_{FH}$ than for the $^3J_{HH}$ couplings. In addition, the different effect of the substituents bonded to the carbon with the coupled proton or to the carbon with the coupled fluorine (*26*) makes the study of the $^3J_{FH}$ couplings an interesting theoretical subject which can give important information about the behavior of heteronuclear coupling constants.

In a previous work (*26*), *ab initio* calculations were applied to the study of $^3J_{FH}$ for the parent molecule of fluoroethane and for di- and trifluoroethane derivatives. In that work the models and equations initially proposed for the substituent effects upon the $^3J_{HH}$ couplings (*27*) were extended to the fluorine–proton couplings. In this paper the equations are extended in order to

[1] To whom correspondence should be addressed.

1090-7807/98 $25.00

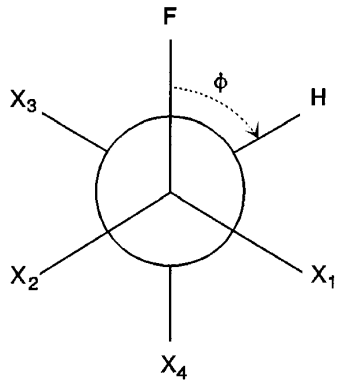

FIG. 1. Numbering for the position of substituents with respect to the coupled nuclei.

include substituent parameters (see under Methods) and the dependence of the Fourier coefficients on the Huggins relative electronegativity (*28*) (see Eqs. [5] and [6]) is investigated both theoretically and empirically (see under Results).

The adopted notation (*26*) is illustrated in Fig. 1. The position of substituents is defined as positive for S_1 and S_3 and negative for S_2 and S_4. The shorthand notation S_1S_2/S_3S_4 indicates the position of substituents with respect to the coupled nuclei. A slash separates a pair of geminal substituents from its neighboring pair. The first two substituents S_1 and S_2 are bonded to the carbon attached to the coupled fluorine and S_3 and S_4 are bonded to the carbon attached to the coupled hydrogen.

MODEL AND EQUATIONS

Vicinal fluorine hydrogen couplings ${}^3J_{\mathrm{FH}}^{X_1X_2/X_3X_4}$ in a (X_1X_2/X_3X_4)-substituted fluoroethane ($\mathrm{CF}X_1X_2$–$\mathrm{CH}X_3X_4$) can be represented as a truncated Fourier series in the fluorine–proton torsion angle ϕ (F–C–C–H) of the form

$$ {}^3J_{\mathrm{FH}}^{X_1X_2/X_3X_4}(\phi) = C_0^{X_1X_2/X_3X_4} + \sum_{n=1}^{m}(C_n^{X_1X_2/X_3X_4}\cos n\phi + S_n^{X_1X_2/X_3X_4}\sin n\phi). \quad [1]$$

In a two-substituent interaction model (*26*), the Fourier coefficients $K_n^{X_1X_2/X_3X_4}$ ($K = C$ or S) are approximated by the linear expression

$$ K_n^{X_1X_2/X_3X_4} = K_n^0 + \sum_i \Delta K_{ni}^{X_i} + \sum_{j>i} \delta K_{nij}^{X_iX_j}, \quad [2]$$

where K_n^0 are the coefficients for the unsubstituted fluoroethane; $\Delta K_{ni}^{X_i}$ corresponds to the effect of a substituent X_i in position i which is defined (*26*) as

$$ \Delta C_{ni}^{X_i} = C_{ni}^{X_i} - C_n^0 \quad \text{and} \quad \Delta S_{ni}^{X_i} = S_{ni}^{X_i}, \quad [3]$$

and the terms $\delta K_{nij}^{X_iX_j}$ correspond to the interaction between a substituent X_i in position i and a substituent X_j in position j,

$$ \delta K_{nij}^{X_iX_j} = K_{nij}^{X_iX_j} - (K_n^0 + \Delta K_{ni}^{X_i} + \Delta K_{nj}^{X_j}), \quad [4]$$

where $K_{nij}^{X_iY_j}$ is the Fourier coefficients of Eq. [1] in a X_iX_j-disubstituted fluoroethane.

In order to reduce the number of parameters to be handled, the individual substituent effects, $\Delta K_n^{X_i}$, and the interactions between substituents, $\delta K_{nij}^{X_iX_j}$, are now translated into substituent parameter relations by means of Taylor series (*26*):

$$ \Delta K_{ni}^{X_i} = k_{ni}^0 + k_{ni}\lambda_{X_i} + k_{nii}\lambda_{X_i}^2, \quad [5]$$

$$ \delta K_{nij}^{X_iY_j} = k_{nij}^0 + k_{nij}^i\lambda_{X_i} + k_{nij}^j\lambda_{Y_j} + k_{nij}\lambda_{X_i}\lambda_{Y_j}. \quad [6]$$

The substituent parameter λ_{X_i} usually has been identified with the Huggins relative electronegativities (*28*) $\lambda_{X_i} = \Delta\chi_{X_i} = \chi_{X_i} - \chi_{\mathrm{H}}$, but the anterior formulation is validated for any other substituent parameter scale (*29*). Allowing for the isodynamic operations (see Eqs. [7] and [14–15] in (*26*)) and considering only terms corresponding to the individual substituent effects (Eq. [5]), the following general expressions for the Fourier coefficients of Eq. [1] are obtained:

$$ C_n^{X_1X_2/X_3X_4} = c_n^0 + c_{n1}^0(\delta_1 + \delta_2) + c_{n1}(\chi_{X_1} + \chi_{X_2}) + c_{n11}(\chi_{X_1}^2 + \chi_{X_2}^2) + c_{n3}^0(\delta_3 + \delta_4) + c_{n3}(\chi_{X_3} + \chi_{X_4}) + c_{n33}(\chi_{X_3}^2 + \chi_{X_4}^2) \quad [7]$$

$$ S_n^{X_1X_2/X_3X_4} = s_{n1}^0(\delta_1 - \delta_2) + s_{n1}(\chi_{X_1} - \chi_{X_2}) + s_{n11}(\chi_{X_1}^2 - \chi_{X_2}^2) + s_{n3}^0(\delta_3 - \delta_4) + s_{n3}(\chi_{X_3} - \chi_{X_4}) + s_{n33}(\chi_{X_3}^2 - \chi_{X_4}^2). \quad [8]$$

Here the delta function δ_i is set equal to 1 when the position i is substituted (nonhydrogen substituent). Otherwise, δ_i is set equal to 0.

With $m = 3$, Eq. [1] has four C_n and three S_n Fourier coefficients. When these seven coefficients in Eq. [1] are substituted by those of Eqs. [7] and [8], a total of forty-six coefficients to be determined theoretically or empirically will result. Obviously, empirical parameterization of a such equation is not feasible and theoretical studies to find out the magnitude of the most important terms should be done in advance. For $m = 2$, the number of coefficients to be determined is reduced to thirty-three.

From the point of view of an empirical parameterization, and owing to the relative small value of the calculated K_3 coefficients in Eq. [1], a value of $m = 2$ will lead, in principle, to an extended Karplus equation sufficiently accurate for practical

purposes. The contributions from terms of higher order and from other secondary factors, such as the effects of changes in bond lengths and bond angles, β-substituent effects, etc., are difficult to evaluate at the moment.

The contributions from the interaction between substituents, not included in Eqs. [7] and [8], are not negligible when two or more substituents are very electronegative (*26*). Considering that the estimation of these effects in an empirical parameterization is quite difficult and that in $^3J_{HH}$ couplings the substituent interaction is reproduced with the cross term $k_{nij}\lambda_{X_i}\lambda_{X_j}$ (see Eq. [6]) (*30*), then, the terms to be added to Eqs. [7] and [8], in order to take into account the substituent interaction, are at least

$$\delta C_n^{X_1X_2/X_3X_4} = c_{n12}(\chi_{X_1}\chi_{X_2}) + c_{n34}(\chi_{X_3}\chi_{X_4}) + c_{n13}(\chi_{X_1}\chi_{X_3} + \chi_{X_2}\chi_{X_4}) + c_{n14}(\chi_{X_1}\chi_{X_4} + \chi_{X_2}\chi_{X_3}) \quad [9]$$

$$\delta S_n^{X_1X_2/X_3X_4} = s_{n13}(\chi_{X_1}\chi_{X_3} - \chi_{X_2}\chi_{X_4}) + s_{n14}(\chi_{X_1}\chi_{X_4} - \chi_{X_2}\chi_{X_3}). \quad [10]$$

These equations will increase the number terms in Eq. [1] to sixty-eight with $m = 3$ and to forty-nine with $m = 2$.

Calculated Couplings Computational Aspects

Several sets of $^3J_{FH}$ values have been calculated at both *ab initio* and semiempirical levels of approximation for 1- and 2-monosubstituted fluoroethanes with substituents CH_3, NH_2, OH, and F. The *ab initio* calculations were carried out at the SCF level (*31–33*) with the SYSMO (System Modena) program using the EOM (equation of motion) (*34*) method at the random phase approximation (RPA) (*35*). Two basis sets were used in the *ab initio* calculations, the standard 6-31G** and a previously defined basis set called B[F–H] (4*s*2*p*1*d*/2*s*1*p*) which include tight *s* functions on the H and F atoms (*26*). For comparison semiempirical calculations were done by means of the INDO/FPT method (*36, 37*) with the use of the program FINITE (*38*). Standard geometries with tetrahedral bond angles and constant bond lengths (*39*) were used. In this way the contributions from changes in local geometry are removed, and the calculated couplings can be used to study the angular dependence and the individual substituent effects. The coupling constants were calculated as a function of the F–H torsional angle ϕ which was driven in 30° steps over the minimum range necessary to cover a complete rotation, allowing for symmetry where appropriate. The K_n coefficients in Eq. [1] were calculated from the theoretical $^3J_{FH}$ values by Fourier inversion (*10*). The CH_3, NH_2, and OH substituents were constrained to staggered conformations. In the case of the NH_2 and OH substituents the coupling constants were calculated for the three staggered orientations. The reported values correspond to the average of these three staggered conformations.

The four contributions, Fermi contact (FC), spin dipolar (SD), orbital diamagnetic (OD), and orbital paramagnetic (OP), to the total $^3J_{FH}^{TO}$ coupling were obtained,

$$^3J_{FH}^{TO} = {}^3J_{FH}^{FC} + {}^3J_{FH}^{SD} + {}^3J_{FH}^{OP} + {}^3J_{FH}^{OD}. \quad [11]$$

The OP and OD contributions were calculated only with the 6-31G** basis set. Owing to the small values of the non-Fermi contact (NC) contributions these are described together. The corresponding contribution are indicated by a superscript when necessary either in the couplings or in the Fourier coefficients.

Data Set of Experimental Couplings

A selected data set consisting of 58 coupling constants $^3J_{FH}$ from 46 compounds was collected from the literature (*40–61*) with a double purpose: to check the theoretical calculations and to parameterize extended Karplus equations. The selected data set comprises molecules with fragments F–C–C–H mono- and pol-substituted. Fragments F–C–C–H with more than one high electronegative substituent (F, O, Cl, N, or Br) were not included in the data set in order to reduce the contribution from the interaction substituent effects $\delta K_{nij}^{X_iY_j}$ (Eq. [6]) that are not included in the parameterization. The data set was restricted to molecules with accurately known conformer populations. The selected molecules are: (i) six-membered rings that can be assumed to exist in a single conformation (with holding groups and/or analyzed at low temperature) or in two energetically equivalent conformers owing to molecular symmetry; (ii) 1-mono- and 1,1-di-fluoroethane derivatives with three energetically equivalent conformers; and (iii) acenaphthene and norbornane derivatives which were included to avoid the correlation between the Fourier coefficients C_1 with C_2 and S_1 with S_2 which appears when the data set is biased toward torsion angles around 60°, 180°, and 300° (see Eq. [10] in (*10*)). In norbornane derivatives, the endo–endo $^3J_{FH}$ couplings were excluded due to the so-called Barfield effect (*62*) present in these kinds of compounds. The experimental coupling constants are a wide range (from 1.9 to 44.4 Hz). The experimental error is smaller than 0.2 Hz for most of the values of the data set. In order to avoid different solvent effects (*63*), molecules analyzed in CCl_3D were selected as long as possible.

Fluorine–proton torsion angles ϕ, a required molecular parameter, are not accurately known for molecules in solution. However, the molecular mechanics method seems to be

TABLE 1

Fourier Coefficients $C_n^{0,MN}$, Eq. [1], Calculated with the Indicated *ab Initio* and Semiempirical Methods in Fluoroethane

Method	*MN*	$C_0^{0,MN}$	$C_1^{0,MN}$	$C_2^{0,MN}$	$C_3^{0,MN}$
INDO	FC	22.75	−9.05	21.85	−0.40
6-31G**	FC	17.56	−8.48	19.81	0.14
B[F–H]	FC	22.72	−11.13	26.85	−0.89
6-31G**	TO	16.94	−7.58	18.87	0.03
B[F–H][a]	TO	22.07	−10.23	25.89	−1.01

Note. Standard geometries were used.

[a] The OP and OD contributions were calculated with the 6-31G** basis set.

TABLE 2

Contributions $\Delta K_{n1}^{X,MN}$ to the Fourier Coefficients, Eq. [3], Hz, in Monosubstituted Fluoroethane Derivatives $CHFXCH_3$ (set-1) Calculated by *ab Initio* (6-31G and B[F–H] Basis Sets) and Semiempirical (INDO/FPT) Methods**

		$\Delta C_{01}^{X,MN}$		$\Delta C_{11}^{X,MN}$		$\Delta C_{21}^{X,MN}$		$\Delta C_{31}^{X,MN}$		$\Delta S_{11}^{X,MN}$		$\Delta S_{21}^{X,MN}$		$\Delta S_{31}^{X,MN}$	
Method	*X*	FC	TO	FC	TO	FC	TO	FC	TO	FC	TO	FC	TO	FC	TO
INDO/FPT	CH_3	−2.41		0.02		−2.32		0.04		−0.27		0.82		0.03	
	NH_2	−2.67		−1.34		−2.77		0.03		−0.86		3.54		0.00	
	OH	−2.04		−1.98		−2.44		0.02		−1.09		4.52		−0.02	
	F	−1.56		−2.32		−2.28		0.00		−1.21		5.16		−0.04	
6.31G**	CH_3	−2.75	−2.80	0.18	0.21	−2.63	−2.52	−0.11	−0.07	−0.31	−0.26	0.76	0.64	0.09	0.03
	NH_2	−4.08	−4.36	−0.56	−0.67	−4.50	−4.41	−0.12	−0.10	−0.62	−0.72	2.75	2.51	0.17	0.10
	OH	−3.78	−4.25	−1.24	−1.44	−4.89	−4.84	−0.04	−0.04	−0.94	−1.19	3.77	3.42	0.14	0.07
	F	−2.86	−3.47	−1.66	−1.93	−4.88	−4.86	0.04	0.03	−1.18	−1.57	4.40	3.99	0.13	0.06
B[F–H][a]	CH_3	−2.45	−2.49	0.06	0.09	−2.61	−2.50	−0.01	0.03	−0.13	−0.07	1.10	0.98	0.05	−0.01
	NH_2	−4.16	−4.42	−0.63	−0.74	−4.87	−4.77	0.04	0.07	−0.19	−0.28	3.48	3.23	0.24	0.17
	OH	−3.76	−4.22	−1.29	−1.50	−5.30	−5.25	0.11	0.12	−0.38	−0.63	4.63	4.27	0.33	0.26
	F	−2.83	−3.43	−1.82	−2.10	−5.36	−5.34	0.14	0.13	−0.63	−1.02	5.27	4.83	0.37	0.30

Note. Standard geometries were used. The FC contributions and TO values are reported.
[a] The OP and OD contributions were calculated with the 6-31G** basis set.

a suitable procedure to calculate reliable geometries for those types of molecules for which appropriated force fields are available. The torsional angles ϕ utilized with the empirical data set were determined using the MM3 force field (*64*).

Both data sets, experimental and calculated, are used to fit the equations described in the section of model and equations. The optimized parameters for these equations were obtained via a standard least-squares procedure.

RESULTS AND DISCUSSION

Calculated Individual Substituent Effects

The calculated Fourier coefficients $C_n^{0,MN}$ (Eq. [1]) for fluoroethane are presented in Table 1. These calculations have been discussed in a previous work (*26*) and are presented here for completeness and for calculating the absolute values of $K_{ni}^{X_i}$ (see Eq. [3]) with the relative substituent effects $\Delta K_{ni}^{X_i}$ pre-

TABLE 3

Contributions $\Delta K_{n3}^{X,MN}$ to the Fourier Coefficients, Eq. [3], Hz, in Monosubstituted Fluoroethane Derivatives CH_2FCH_2X (set-2) Calculated by *ab Initio* (6-31G and B[F–H] Basis Sets) and Semiempirical (INDO/FPT) Methods**

		$\Delta C_{03}^{X,MN}$		$\Delta C_{13}^{X,MN}$		$\Delta C_{23}^{X,MN}$		$\Delta C_{33}^{X,MN}$		$\Delta S_{13}^{X,MN}$		$\Delta S_{23}^{X,MN}$		$\Delta S_{33}^{X,MN}$	
Method	*X*	FC	TO	FC	TO	FC	TO	FC	TO	FC	TO	FC	TO	FC	TO
INDO/FPT	CH_3	−2.05		1.97		−1.54		0.44		−0.91		1.28		−1.12	
	NH_2	−2.14		1.13		−2.20		0.41		−1.62		3.58		−1.03	
	OH	−2.23		0.52		−2.81		0.32		−1.82		4.43		−0.74	
	F	−3.11		0.45		−3.88		0.23		−1.99		5.25		−0.58	
6.31G**	CH_3	−3.30	−3.15	2.03	2.06	−3.04	−3.08	0.27	0.28	−1.24	−1.05	2.11	2.09	−0.82	−0.85
	NH_2	−4.32	−4.22	1.20	1.23	−4.69	−4.67	0.06	0.09	−1.52	−1.31	5.18	5.23	−0.41	−0.45
	OH	−4.35	−4.41	0.11	0.16	−5.49	−5.40	−0.26	−0.23	−1.65	−1.46	6.63	6.75	0.01	−0.05
	F	−4.29	−4.42	−0.84	−0.81	−6.08	−5.94	−0.57	−0.54	−1.62	−1.46	7.39	7.57	0.42	0.36
B[F–H][a]	CH_3	−3.70	−3.55	4.32	4.35	−3.76	−3.80	1.33	1.33	−2.27	−2.08	3.05	3.04	−2.05	−2.08
	NH_2	−5.43	−5.34	3.88	3.90	−6.13	−6.10	1.57	1.59	−2.80	−2.58	6.64	6.69	−2.16	−2.20
	OH	−6.03	−6.10	2.75	2.79	−7.33	−7.24	1.40	1.43	−2.93	−2.73	8.30	8.42	−1.82	−1.87
	F	−6.68	−6.82	1.78	1.80	−8.28	−8.13	1.21	1.24	−2.84	−2.68	9.30	9.48	−1.45	−1.51

Note. Standard geometries were used. The FC contributions and TO values are reported.
[a] The OP and OD contributions were calculated with the 6-31G** basis set.

sented in Tables 2 and 3 for both sets of molecules, 1- and 2-substituted fluoroethane derivatives, respectively. The substituent effects $\Delta K_{ni}^{X_i}$ have been represented against the Huggins relative electronegativity $\Delta\chi_{X_i}$ in Figs. 2 and 3. The curves plotted in these figures correspond to the fitted quadratic Eq. [5]. In Table 4, a selection of the best (lower rms deviation) fits of $\Delta K_{ni}^{X_i}$ against the Huggins relative electronegativities $\Delta\chi_{X_i}$ using different sets of terms in equations is given. It is termed set-1 to the 1-substituted fluoroethane derivatives and set-2 to the 2-substituted ones. Owing to the differences found for both sets, these are discussed separately.

1. Substituted fluoroethane derivatives. For set-1, when the substituent is bonded to the carbon attached to the coupled fluorine, there are not large differences, concerning the substituent effects ΔK_{n1}^{X}, between the results of both *ab initio* basis sets, the 6-31G** and the B[F–H]. For the largest effects, ΔC_{01}^{X}, ΔC_{21}^{X}, and ΔS_{21}^{X}, a quadratic dependence upon the substituent electronegativity $\Delta\chi_X$ is obtained (see Fig. 2). The best fits of these coefficients to Eq. [5] require the linear and quadratic terms, k_{01} and k_{n11}, and in the case of ΔS_2^X also the independent term s_{n1}^0 must be included; see Table 4. A similar representation for the vicinal proton–proton couplings $^3J_{HH}$ led us to suggest (*65*) a quadratic or exponential dependence on $\Delta\chi_X$ for ΔK_{01}^{X}. However, for the $^3J_{FH}$ couplings, it is found that

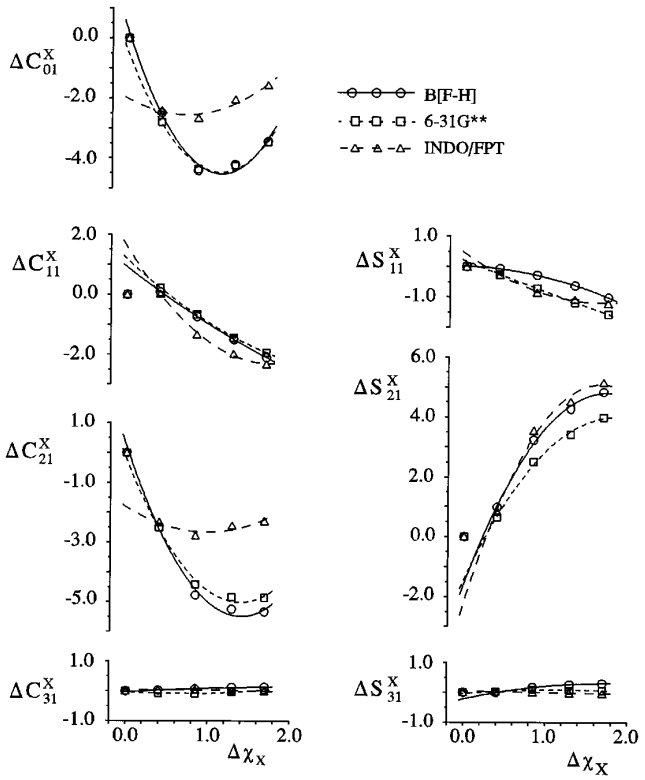

FIG. 2. Calculated B[F–H] (○), 6-31G** (□), and INDO/FPT (△) contributions ΔK_n^X, Hz, for the effects of an individual substituent X to the Fourier coefficient K_n^X in $CHFX–CH_3$ molecules (set 1) as a function of the relative electronegativities $\Delta\chi_X$.

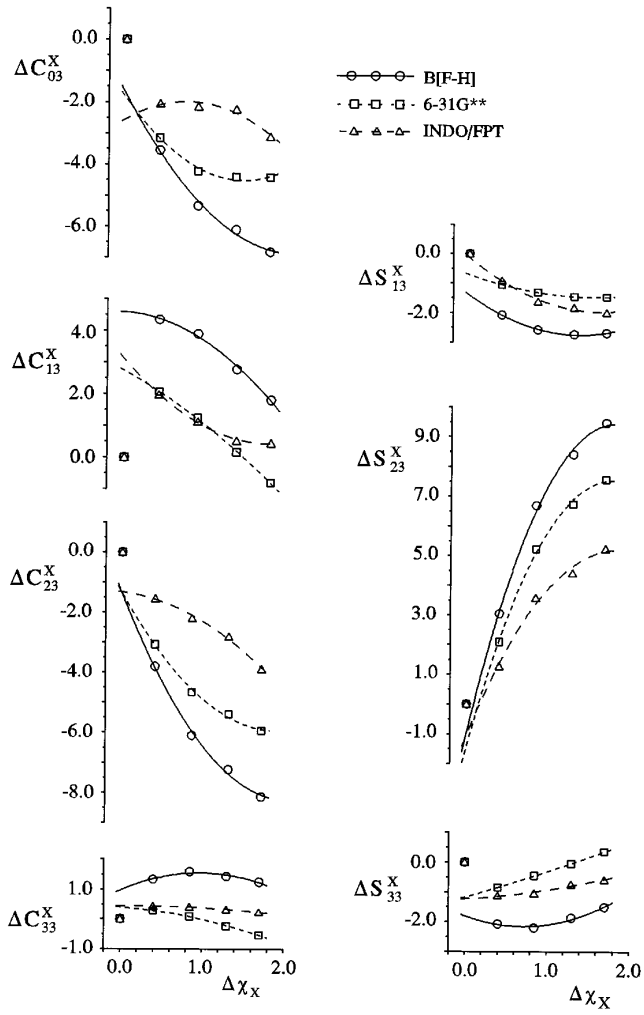

FIG. 3. Calculated B[F–H] (○), 6-31G** (□), and INDO/FPT (△) contributions ΔK_n^X, Hz, for the effects of an individual substituent X to the Fourier coefficient K_n^X in $CH_2F–CH_2X$ molecules (set 2) as a function of the relative electronegativities $\Delta\chi_X$.

the representations of ΔC_{01}^{X} and ΔC_{21}^{X} against $\Delta\chi_X$ present a minimum; i.e., for high electronegativities these contributions increase with the relative substituent electronegativity. It should be noted that to corroborate empirically this rare effect is difficult owing to the reactivity of 1-fluoroethane derivatives when there is an electronegative substituent geminal to the fluorine. For the smaller effects ΔC_{11}^{X} and ΔS_{11}^{X}, a slightly quadratic dependence is observed but from a practical point of view a linear dependence can be assumed. The ΔC_{31}^{X} and ΔS_{31}^{X} are smaller in magnitude than 0.14 and 0.30 Hz and can be neglected.

The non-Fermi contact contributions $(\Delta K_{n1}^{X,\mathrm{TO}} - \Delta K_{n1}^{X,\mathrm{FC}})$ increase in magnitude with the substituent electronegativity except ΔC_{21}^{X} and the less important coefficients ΔC_{31}^{X} and ΔS_{31}^{X} (see Table 2). The largest NC contribution (0.6 Hz) corresponds to $\Delta C_{01}^{F,\mathrm{NC}}$ in 1,1-difluoroethane.

The INDO/FPT results for ΔC_{01}^{X} and ΔC_{21}^{X} are qualitatively

TABLE 4

Selected Results from the Fits of the Calculated Individual Substituent Effects $\Delta K_{ni}^{X,TO}$ to Eq. [5] with Different Number of Coefficients[a] and Using Huggins' Relative Electronegativities (*28*) as Substituent Parameter

Set-1 ($CHFX–CH_3$)

Coeff.	ΔC_{01}^X		ΔC_{11}^X		ΔC_{21}^X		ΔS_{11}^X	ΔS_{21}^X
k_{n1}^0		0.2 (0.8)	0.7 (0.1)	0.9 (0.0)		0.2 (0.8)		−1.6 (0.4)
k_{n1}	−7.9 (0.4)	−8.3 (1.7)	−1.7 (0.1)	−2.1 (0.0)	−7.6 (0.4)	−8.0 (1.7)		7.3 (1.0)
k_{n11}	3.5 (0.3)	3.6 (0.8)		0.2 (0.0)	2.7 (0.3)	2.8 (0.8)	−0.4 (0.0)	−2.1 (0.5)
σ^b	0.22	0.30	0.05	0.01	0.22	0.30	0.02	0.17
$\Delta_{max}{}^c$	0.22	0.21	0.04	0.01	0.22	0.21	0.02	0.12

Set-2 ($CH_2F–CH_2X$)

Coeff.	ΔC_{03}^X		ΔC_{13}^X	ΔC_{23}^X	ΔC_{33}^X	ΔS_{13}^X	ΔS_{23}^X	ΔS_{33}^X
k_{n3}^0	−2.9 (0.5)	−1.7 (0.6)	4.5 (0.1)	−1.4 (0.6)	1.0 (0.2)	−1.4 (0.1)	−1.0 (0.7)	−2.4 (0.2)
k_{n3}	−2.4 (0.4)	−5.2 (1.3)		−6.8 (1.3)	1.2 (0.4)	−1.9 (0.2)	11.6 (1.6)	0.5 (0.2)
k_{n33}		1.3 (0.6)	−1.0 (0.1)	1.7 (0.6)	−0.6 (0.2)	0.7 (0.1)	−3.2 (0.8)	
σ^b	0.38	0.23	0.10	0.22	0.08	0.03	0.29	0.19
$\Delta_{max}{}^c$	0.40	0.15	0.11	0.15	0.05	0.02	0.20	0.19

[a] Estimated errors in parentheses.
[b] Root mean square deviation.
[c] Maximum deviation.

different from those obtained with the *ab initio* methods. However, an increase of these coefficients with the substituent electronegativity is also observed for the substituents OH and F (see Fig. 2). Similar semiempirical results were graphically presented by Govil (*17*). For the remaining substituent effects the INDO/FPT results agree quite well with the *ab initio* ones (see, for instance, the graph for the coefficient ΔS_{21}^X).

2. Substituted fluoroethane derivatives. The *ab initio* calculated substituent effects ΔK_{n3}^X for set-2, when the substituent is bonded to the carbon attached to the coupled proton, show some qualitative differences for the two used basis sets, but both trends are similar. The contributions ΔK_{n3}^X calculated with the B[F–H] basis set are the largest in magnitude, and those calculated with the 6-31G** basis set are, in general, between the B[F–H] and the INDO/FPT ones. The trends for set-2 are comparable to those found for the $^3J_{HH}$ couplings (*10*, *65*); i.e., the dependence on $\Delta\chi_X$ for the largest effects ΔC_{03}^X, ΔC_{13}^X, ΔC_{23}^X, and ΔS_{23}^X, is quadratic or exponential (see Fig. 3 and Table 4).

Two points are remarkable from Figs. 2 and 3 and from Table 4: (i) quadratic coefficients k_{nii} are found in the representation of ΔC_0^X, ΔC_2^X, and ΔS_2^X against $\Delta\chi_X$, for both kinds of substitution (set-1 and set-2) and (ii) a gap exists between the Fourier coefficients of the parent molecule, fluoroethane, and those belonging to second row substituents. This gap is more significant in the set-2, where in order to reproduce the calculated substituent effects ΔK_{03}^X the terms k_{03}^0 must be included in Eq. [5] (see Table 4). A similar gap was detected for the $^3J_{HH}$ couplings (*65*).

The variation with the electronegativity of the non-Fermi contribution is smaller than that of set-1, corresponding the largest NC contribution (0.21 Hz) to $\Delta S_{13}^{NH_2,NC}$ in 2-fluoroethylamine.

Fits to Experimental Couplings

A set of experimental $^3J_{FH}^{exp}$ values selected from the literature is given in Table 5. These couplings were used to parameterize the equation resulting after substitution in Eq. [1] of coefficients C_n and S_n by Eqs. [7] and [8] and using different number of coefficients. In addition, the set of 108 values of $^3J_{FH}$ calculated with the B[F–H] basis set were fitted with the same number of coefficients to compare the results. The calculated $^3J_{FH}$ couplings of fluoroethylamine and fluoroethanol used in the fits are the average couplings for the three staggered positions of the $-NH_2$ and $-OH$ groups. Only total (TO) couplings were used in the fits. A selection of results is presented in Table 6.

First, the coupling constants were fitted to a simple Karplus-type equation obtaining a rms deviation of 5.5/5.2 Hz and a maximum deviation of 12.2/15.7 Hz for the experimental/calculated couplings. The Fourier coefficients c_0, c_1, and c_2 obtained from the experimental couplings (16.8, −3.8, and 12.0 Hz) present important differences from the theoretical ones (18.2, −9.3, and 21.1 Hz). The differences between the experimental and calculated coefficients can be attributed, in part, to the fact that both data sets cover differently the space of variables and, therefore, the coefficients include implicitly the substituent effects in a different way.

TABLE 5
Data Set of Experimental Coupling Constants $^3J_{FH}^{exp}$

Compound	$^3J_{FH}^{exp}$	$^3J_{FH}^{est}$	ϕ_{FCCH}[a]	$[S_1S_2/S_3S_4]$	Ref.
Fluoroethane[b]	26.4	25.1	Average	HH/HH	(*40*)
1,1-Difluoroethane	20.8	19.1	Average	FH/HH	(*41*)
1-Bromofluoroethane[c]	21.0	22.5	Average	BrH/HH	(*42*)
2-Fluoropropane	23.7	23.7	Average	CH/HH	(*41*)
2,2-Difluoropropane[d]	17.6	17.7	Average	CF/HH	(*43*)
2-Fluoro-2-methylpropane	21.3	22.3	Average	CC/HH	(*44*)
Axial fluorocyclohexane[d]	10.0	11.8	−56.5	CH/HC	(*45*)
	44.0	44.0	−172.9	CH/CH	
4-*tert*-Butyl-1,1-difluorocyclohexane[e]	34.3	34.3	−173.7	CF/CH	(*40*)
	11.5	11.3	−57.1	CF/HC	
3-Methyl-1,1-difluorocyclohexane[e]	34.1	34.4	−173.9	CF/CH	(*40*)
	10.2	11.0	−57.6	CF/HC	
cis-1-Fluoro-2-chlorocyclohexane[c]	30.0	30.4	−176.2	CH/CCl	(*46*)
2-Fluoro(ax)-3,3,5,5-tetramethyl-*cis*-cyclohexanol[c]	27.0	27.1	177.2	HC/OC	(*47*)
2-Fluoro(ec)-6-bromine-3,3,5,5-tetramethyl-*cis*-cyclohexanol[c]	12.6	12.7	57.8	HC/OC	(*47*)
trans-4-*tert*-Butyl-*cis*-2-fluorocyclohexanol[f]	44.4	44.1	−174.1	CH/CH	(*48*)
trans-4-*tert*-Butyl-*cis*-2-fluoro-1-cyclohexylmethyl ether	29.1	27.1	177.2	HC/OC	(*48*)
	43.6	44.2	−174.8	CH/CH	
Tetra-O-acetyl-2-deoxy-2-fluoro-β-D-glucopyranose	14.2	13.9	−52.1	HC/CO	(*49*)
Tetra-O-acetyl-2-deoxy-2-fluoro-α-D-mannopyranose	24.5	26.3	−174.3	CH/CO	(*49*)
Tetra-O-acetyl-2-deoxy-2-fluoro-β-D-mannopyranose	25.6	26.8	−176.1	CH/CO	(*49*)
Tetra-O-acetyl-2-deoxy-2-fluoro-α-D-glucopyranose	11.5	12.7	−56.4	HC/CO	(*50*)
Tetra-O-acetyl-3-deoxy-3-fluoro-β-D-glucopyranose	12.8	13.8	−52.5	HC/CO	(*51*)
	12.8	14.6	49.3	CH/OC	
Tetra-O-acetyl-3-deoxy-3-fluoro-α-D-glucopyranose	12.5	14.2	−51.1	HC/CO	(*51*)
	12.5	14.3	50.6	CH/OC	
4-Deoxy-4-fluoro-β-D-glucose	14.5	13.6	53.1	CH/OC	(*52*)
4-Deoxy-4-fluoro-α-D-glucose	15.0	13.4	54.0	CH/OC	(*53*)
2-Deoxy-2-iodo-α-D-mannopyranosyl	3.5	4.7	−56.1	OH/IC	(*54*)
Triacetate-2-deoxy α-D-glucose fluoride	5.0	5.1	56.5	HO/CH	(*55*)
3,4,6-Tri-O-acetyl-2-deoxy-2-fluoro-β-D-*gluco*-pyranosylfluoride	15.0	14.6	−49.5	HC/CO	(*56*)
3,4,6-Tri-O-acetyl-2-deoxy-2-fluoro-α-D-*manno*-pyranosylfluoride	27.0	26.3	−174.2	CH/CO	(*56*)
2-*iso*-Propyl 5-fluoro-*axial*-1,3-dioxolane	36.9	36.6	−166.6	CH/OH	(*57*)
	18.0	16.4	−48.1	CH/HO	
3,4,6-Tri-O-acetyl-2-deoxy-2-fluoro-α-D-manno-pyranosylfluoride	15.0	14.2	−50.9	HC/CO	(*58*)
	13.5	14.6	49.3	CH/OC	
2,4,6-Tri-O-acetyl-3-deoxy-3-fluoro-α-D-gluco-pyranosylfluoride	14.5	13.3	−54.2	HC/CO	(*58*)
	13.5	14.7	49.0	CH/OC	
2,3,6-Tri-O-acetyl-4-deoxy-4-fluoro-β-D-gluco-pyranosylfluoride	15.8	13.7	52.7	CH/OC	(*59*)
	4.9	5.3	−56.7	HC/OC	
2,3,6-Tri-O-acetyl-4-deoxy-4-fluoro-α-D-gluco-pyranosylfluoride	14.6	13.8	52.6	CH/OC	(*59*)
1-Fluoro-acenaphthene[f]	29.5	29.5	−10.6	HC/CH	(*60*)
1,1-Bromofluoro-acenaphthene[f]	23.0	23.8	−12.6	BrC/CH	(*60*)
	10.0	9.4	108.6	BrC/HC	
cis-1,2-Bromofluoro-acenaphthene[f]	21.5	21.6	9.3	CH/BrC	(*60*)
1-Chloro-1-fluoro-acenaphthene[f]	32.8[g]	30.9	−11.3, 109.9	ClC/CH	(*60*)
1-Chloro-1-fluoro-acenaphthene[f]	10.0	9.5	109.4	HC/ClC	(*60*)
trans-1,2-Chlorofluoro-acenaphthene[f]	21.0	20.3	9.6	CH/ClC	(*60*)
cis-1,2-Iodochloro-1-fluoro-acenaphthene[f]	6.0	5.8	100.4	ClC/IC	(*60*)
cis-1,2-Dichloro-1-fluoro-acenaphthene[f]	19.7	18.7	−18.1	CCl/IC	(*60*)
1,1-Difluoro-acenaphthene[f]	26.4[g]	26.6	0.3, 121.5	FC/HC	(*60*)
trans-1,2-Difluoro-acenaphthene[f]	18.8	18.4	18.0	CH/FC	(*60*)
cis-1,2-Difluoro-acenaphthene[f]	5.2	3.4	122.8	HC/FC	(*60*)
1,1-Difluoro-2-iodo-acenaphthene[f]	16.0	16.7	−19.4	CF/IC	(*60*)
cis-1,2-Difluoro-1-methyl-acenaphthene[f]	22.0	22.3	Average	CC/HH	(*60*)
Hexachlorocyclopentadiene-*cis*-1,2-difluoroethylene[c]	1.9	3.2	−121.7	CH/CF	(*61*)
Hexachlorocyclopentadiene 1,1-difluoroethylene[c]	7.4	7.0	−122.3	CF/CH	(*61*)
	4.5	5.5	118.8	FC/HC	

Note. The estimated values $^3J_{FH}^{est}$ were calculated with Eq. [12]. The torsional angles ϕ_{FCCH} were determined with the MM3 method. $[S_1S_2/S_3S_4]$ indicate the position of substituents (see Fig. 1). Except when indicated, the solvent is CCl_3D.

[a] Average means that the coupling corresponds to the average of three energetically equivalent conformers.
[b] $CCl_4/CDCl_3$.
[c] CCl_4.
[d] neto.
[e] $CFCl_3/CDCl_3$.
[f] $CFCl_3$.
[g] The experimental coupling corresponds to the sum of the couplings for the two torsional angles.

TABLE 6

Results for the Fits of the Experimental and Calculated Data Sets of $^3J_{FH}$ Couplings to Eqs. [1] and [5] with Different Number of Coefficients and Using Huggins' Relative Electronegativities as Substituent Parameters

	Karplus-type		Fit A		Fit B	
Coefficients	Exp.	Calc.	Exp.	Calc.	Exp.	Calc.
c_0	16.8 (0.7)	18.2 (0.5)	24.8 (0.8)	20.4 (0.4)	25.1 (0.7)	20.4 (0.4)
c_1	−3.8 (1.1)	−9.3 (0.7)	−6.8 (1.1)	−8.5 (0.6)	−7.0 (1.0)	−8.5 (0.6)
c_2	12.0 (1.3)	21.1 (0.7)	18.3 (1.3)	24.4 (0.6)	20.2 (1.3)	24.9 (0.7)
c_{01}			−3.3 (0.5)	−1.5 (0.4)	−3.5 (0.5)	−1.5 (0.4)
c_{11}			−0.8 (0.6)	−2.5 (0.6)	−0.8 (0.6)	−2.5 (0.6)
c_{21}			−1.8 (0.7)	−2.7 (0.6)	−1.9 (0.6)	−3.1 (0.6)
s_{11}			−3.4 (0.8)	−0.5 (0.4)	−1.7 (0.8)	−0.5 (0.4)
s_{21}			6.0 (0.7)	3.1 (0.4)	6.1 (0.6)	2.9 (0.9)
c_{03}			−5.5 (0.5)	−3.2 (0.4)	−5.1 (0.5)	−3.2 (0.4)
c_{13}			1.1 (0.8)	0.8 (0.6)	1.2 (0.7)	0.8 (0.6)
c_{23}			−5.7 (0.8)	−4.3 (0.6)	−10.7 (2.0)	−7.8 (2.0)
s_{13}			−3.0 (1.0)	−2.0 (0.4)	−2.2 (0.9)	−2.0 (0.4)
s_{23}			7.0 (0.7)	6.2 (0.4)	6.5 (0.7)	4.8 (0.9)
s^0_{21}					−2.0 (0.7)	0.2 (1.0)
s^0_{23}					−2.0 (0.8)	1.8 (1.0)
c_{233}					3.4 (1.3)	2.12 (1.2)
σ^a	5.50	5.23	1.44	2.12	1.24	2.08
Σ^b	1666	2874	94	425	65	398
$\Delta_{max}{}^c$	12.0	15.7	2.7	6.9	2.0	6.0

Note. The estimated errors are given in parentheses.

[a] rms deviation.

[b] Sum of squares of deviations.

[c] Maximum deviation.

Fit A corresponds to an extended Karplus-type equation which includes substituent effects represented by linear terms (second term of the right-hand part of Eq. [5]). The rms deviations for these fits are 1.4 and 2.1 Hz for the empirical and theoretical couplings, respectively, and the maximum deviations are 2.7 and 6.9 Hz, respectively. Now, the Fourier coefficients c_0, c_1, and c_2 (24.8, −6.8, and 18.3 Hz) obtained from the experimental couplings present a better agreement with those (20.4, −8.5, and 24.4 Hz) obtained from the calculated couplings than in the case of the fits to a Karplus-type equation. The theoretical coefficients corresponding to the substituent effects (k_{ni}) agree roughly with the empirical ones. The four largest coefficients are s_{21} (6.0 (empirical)/3.1 (theoretical)), c_{03} (−5.5/−3.2), c_{23} (−5.7/−4.3), and s_{23} (7.0/6.2). Except c_{11} and c_{21}, the empirical coefficients are larger in magnitude.

Fit B is one of the best fits that we could obtain for the experimental data set. The equation obtained,

$$
\begin{aligned}
{}^3J_{\mathrm{HF}}^{X_1X_2/X_3X_4} = {} & [25.1 - 3.5(\Delta\chi_{X_1} + \Delta\chi_{X_2}) \\
& - 5.1(\Delta\chi_{X_3} + \Delta\chi_{X_4})] + [-7.0 - 0.8(\Delta\chi_{X_1} + \Delta\chi_{X_2}) \\
& + 1.2(\Delta\chi_{X_3} + \Delta\chi_{X_4})]\cos(\phi_{\mathrm{FH}}) \\
& + [20.2 - 1.9(\Delta\chi_{X_1} + \Delta\chi_{X_2}) - 10.7(\Delta\chi_{X_3} + \Delta\chi_{X_4})] \\
& \times \cos(2\phi_{\mathrm{FH}}) + [-1.7(\Delta\chi_{X_1} - \Delta\chi_{X_2}) \\
& - 2.2(\Delta\chi_{X_3} - \Delta\chi_{X_4})]\sin(\phi_{\mathrm{FH}}) + [6.1(\Delta\chi_{X_1} - \Delta\chi_{X_2}) \\
& + 6.5(\Delta\chi_{X_3} - \Delta\chi_{X_4})]\sin(2\phi_{\mathrm{FH}}) + 3.4(\Delta\chi^2_{X_3} + \Delta\chi^2_{X_4}) \\
& \times \cos(2\phi_{\mathrm{FH}}) - [2.0(\delta_1 - \delta_2 + \delta_3 - \delta_4)]\sin(2\phi_{\mathrm{FH}}),
\end{aligned}
\qquad [12]
$$

reproduces the experimental values with a rms deviation of 1.24 Hz and a maximum deviation of 2.0 Hz.[2] The estimated values of $^3J_{\mathrm{FH}}$ calculated with Eq. [12] for the molecules of the experimental data set are shown in the third column of Table 5. Owing to the limited number of experimental couplings, only two independent coefficients (k^0_{ni}) and one quadratic coefficient (k_{nii}) were included in this fit. The introduction of these three coefficients in the equation to be fitted reduces the rms deviation from 1.44 Hz (fit

[2] A simple program (JFH100) which calculates and plots the $^3J_{FH}$ coupling constants with Eq. [12] can be obtained by request from the following e-mail address: jesus.sanfabian@uam.es.

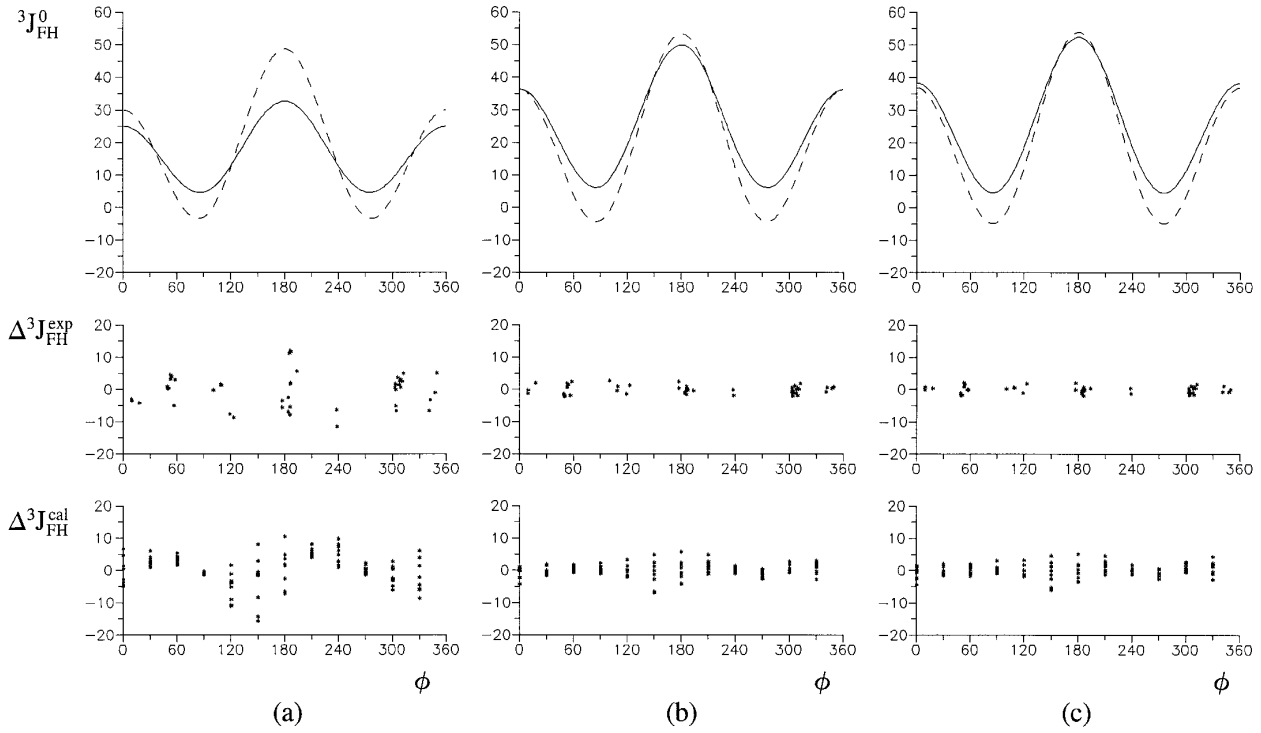

FIG. 4. Illustration of results in Table 6 for three different fits of the $^3J_{FH}$ couplings: (a) Karplus-type, (b) fit A, and (c) fit B. Karplus-type curves of $^3J^0_{FH}$ against the torsion angle ϕ appear in the upper part of figure. The $^3J_{FH}(\phi)$ values are calculated including only the coefficients c_0, c_1, and c_2 derived from experimental data (solid lines) and from calculated data (dashed lines). Deviations between the experimental (and calculated) couplings from those estimated using all the coefficients of the fits in Table 6 appear under the corresponding Karplus-type curves.

A) to 1.24 Hz (fit B). These coefficients are s^0_{21} (−2.0) and s^0_{23} (−2.0) that correspond to the independent term of Eq. [5] and c_{233} (3.4), which is a quadratic correction for the Fourier coefficient C_2 when the substituents are attached to the carbon bonded to the coupled proton. The first two coefficients do not agree with the theoretical ones. It should be noted that only slightly different results for the rms deviation can be obtained by changing an independent or quadratic coefficient by its corresponding quadratic or independent one, respectively. For example, when the coefficient s^0_{21} is replaced by s_{211} the rms deviation increases slightly to 1.26 Hz. The Karplus coefficients (25.1, −7.0, and 20.2 Hz) are closer to the calculated coefficients for fluoroethane (22.1, −10.2, and 25.9 Hz; see Table 1). It should be noted that for our substituent model (*26, 27*) these coefficients should coincide with those of the parent molecule.

Figure 4 illustrates the results in Table 6. In the upper part, the $^3J^0_{FH}$ couplings calculated from the experimental (solid line) and calculated (dashed line) c_0, c_1, and c_2 coefficients are represented against the torsional angles ϕ. These Karplus-type curves correspond to the parent molecule of fluoroethane, i.e., without substituent effects. The experimental and calculated curves are different for the Karplus-type fit, Fig. 4a, where the substituent effects are not accounted for explicitly. However, the differences decrease for fits A and B of Table 6 (Figs. 4b and 4c), which include explicitly the substituent effects. The largest differences between the experimental and calculated curves for fits A and B appear for ϕ around 90° and 270°. The reason could be the lack of experimental $^3J_{FH}$ values for these angles. Below the Karplus-type curve, the deviations Δ^3J_{FH} for the coupling constants estimated using all the coefficients of fits in Table 6 are shown against the torsional angle ϕ. The deviations are large for the Karplus-type fit (Fig. 4a) where the substituent effects are not considered. The deviations are much smaller when the lineal substituent effects are included, fit A (Fig. 4b). The three corrective coefficients s^0_{21}, s^0_{23}, and c_{233} included in the fit B slightly reduce the deviations with respect to the fit A. It is important to note that for the last two fits, the deviations are nearly independent of the torsional angle ϕ.

It should be emphasized that Eq. [12] must be used with prudence and allowing for the simplifying assumptions made in its derivation. The equation does not include the substituent interaction effects and the through space effects such as the Barfield effect (*62*). Consequently, it should be used neither in polysubstituted fluoroethanes with more than one electronegative substituent nor in exo–exo and endo–endo vicinal coupling constants in norbornane and norbornene derivatives. Several other secondary factors, quoted above, are not included in Eq. [12], and, in some situations, their contribution is not negligible. Further improvements on the present formalism will require a deeper insight into the contributions from these secondary factors.

CONCLUSIONS

Different extended Karplus equations which incorporate, in addition the torsional dependence, the electronegativity substituent effects have been formulated for the vicinal fluorine–proton coupling constants. The substituent effects are described following a model that considers both individual substituent and interaction between substituents effects. These effects are developed as a Taylor series in function of substituent parameters. Only the individual substituent effects have been studied in the present work. Larger data sets than the available ones are necessary to analyze the effects of interaction between substituents. In fact, the development of the individual substituent effects by means of a quadratic equation (Eq. [5]) is difficult at the present and only insight about the linear terms can be obtained.

The application of the equations to experimental and calculated data sets of coupling constants is interesting for two reasons. On the one hand, the empirical parameterization of equations is the only procedure by which to obtain a reliable Karplus equation to be used in practice. On the other, the calculated couplings can predict the terms to be included in the Karplus equations and are very useful to overcome, in part, the problems derived from the limited size of the experimental data sets.

In this work, several extended Karplus equations were tested using calculated and experimental data sets. The agreement between the result from both data sets is fairly good for the fits A and B of Table 6 which includes a linear dependence on the substituent electronegativity. The differences may be attributed, in part, to the following reasons: (i) the experimental data set does not cover all the variable space and (ii) the calculated coupling constants are not very accurate owing to the medium size basis sets used and the lack of electronic correlation.

An extended Karplus equation that includes the electronegativity substituent effect (Eq. [12]) has been parameterized from the experimental data set with a rms deviation of 1.2 Hz. Although this equation has some limitations (see above) and it is not a closed solution, it is a useful approximation that can be used to predict the vicinal fluorine–proton coupling constants of fragments with no more than one high electronegative substituent.

ACKNOWLEDGMENTS

This work was supported in part by the Dirección General de Investigación Científica y Técnica of Spain (Proyecto PB94-0161). We express our appreciation to professors P. Lazzeretti, R. Zanasi, and M. Malagoli for providing us with the SYSMO *ab initio* computer programs. Computer time provided by the Centro de Computacion Cientifica of Universidad Autónoma de Madrid is also gratefully acknowledged.

REFERENCES

1. C. Altona, *in* ''Encyclopedia of Nuclear Magnetic Resonance'' (D. M. Grant and R. K. Harris, Eds.), Vol. 8, p. 4909, Wiley, Chichester/New York (1996).
2. W. A. Thomas, *Prog. NMR Spectroc.* **30,** 183 (1997).
3. K. G. R. Pachler, *Tetrahedron Lett.,* 1955 (1970).
4. K. G. R. Pachler, *Tetrahedron* **27,** 187 (1971).
5. K. G. R. Pachler, *J. Chem. Soc. Perkin II,* 1936 (1972).
6. C. A. G. Haasnoot, F. A. A. M. De Leeuw, and C. Altona, *Tetrahedron* **36,** 2783 (1980).
7. W. J. Colucci, S. J. Jungk, and R. D. Gandour, *Magn. Reson. Chem.* **23,** 335 (1985).
8. K. Imai and E. Ōsawa, *Magn. Reson. Chem.* **28,** 668 (1990).
9. J. van Wijk, B. D. Huckriede, J. H. Ippel, and C. Altona, *Methods Enzymol.* **211,** 286 (1992).
10. J. San Fabián, J. Guilleme, E. Díez, P. Lazzeretti, M. Malagoli, R. Zanasi, A. L. Esteban, and F. Mora, *Mol. Phys.* **82,** 913 (1994).
11. M. Karplus, *J. Chem. Phys.* **30,** 11 (1959).
12. M. Karplus, *J. Am. Chem. Soc.* **85,** 2870 (1963).
13. R. J. Abraham, E. J. Chambers, and W. A. Thomas, *Magn. Reson. Chem.* **32,** 248 (1994).
14. W. S. Brey and M. L. Brey, *in* ''Encyclopedia of Nuclear Magnetic Resonance'' (D. M. Grant and R. K. Harris, Eds.), Vol. 3, p. 2063, Wiley, Chichester/New York (1996).
15. K. L. Williamson, Y. F. Li Hsu, F. H. Hall, and S. Swager, *J. Am. Chem. Soc.* **88,** 5678 (1966).
16. K. L. Williamson, Y. F. Li Hsu, F. H. Hall, S. Swager, and M. S. Coulter. *J. Am. Chem. Soc.* **90,** 6717 (1968).
17. G. Govil, *Mol. Phys.* **21,** 953 (1971).
18. M. S. Gopinathan and P. T. Narasimhan, *Mol. Phys.* **21,** 1141 (1971).
19. R. J. Abraham and L. Cavalli, *Mol. Phys.* **9,** 67 (1965).
20. R. J. Abraham, L. Cavalli, and K. G. R. Pachler, *Mol. Phys.* **11,** 471 (1966).
21. A. M. Ihrig and S. L. Smith, *J. Am. Chem. Soc.* **92,** 759 (1970).
22. H. Jensen and K. Schaumburg, *Mol. Phys.* **22,** 1041 (1971).
23. L. D. Hall and D. L. Jones, *Can. J. Chem.* **51,** 2925 (1973).
24. J. W. Emsley, L. Phillips, and V. Wray, *Prog. NMR Spectrosc.* **10,** 83 (1977).
25. S. Hamman, C. Bequin, C. Charlton, and Luu-duc, *Org. Magn. Reson.* **21,** 361 (1983).
26. J. San Fabián and J. Guilleme, *Chem. Phys.* **206,** 325 (1996).
27. E. Díez, J. San Fabián, J. Guilleme, C. Altona, and L. A. Donders, *Mol. Phys.* **68,** 49 (1989).
28. M. L. Huggins, *J. Am. Chem. Soc.* **75,** 4123 (1953).
29. C. Altona, R. Francke, R. Haan, J. H. Ippel, G. J. Daalmans, A. J. A. Westra Hoekzema, and J. van Wijk, *Magn. Reson. Chem.* **32,** 670 (1994).
30. J. Guilleme, J. San Fabián, E. Díez, F. Bermejo, and A. L. Esteban, *Mol. Phys.* **68,** 65 (1989).
31. P. Lazzeretti and R. Zanasi, *J. Chem. Phys.* **77,** 2448 (1982).
32. P. Lazzeretti, *Int. J. Quant. Chem.* **15,** 181 (1979).
33. P. Lazzeretti, *J. Chem. Phys.* **71,** 2514 (1979).
34. C. V. McCurdy, Jr., T. N. Rescigno, D. L. Yaeger, and V. McKoy, ''Methods of Electron Structure Theory'' (H. F. Shaefer, III, Ed.), Vol. 3, p. 339, Plenum, New York (1977).
35. J. Oddershede, *Adv. Quant. Chem.* **11,** 275 (1978).
36. J. A. Pople, J. W. McIver, and N. J. Ostlund, *J. Chem. Phys.* **49,** 2960 (1968).
37. J. A. Pople, D. L. Beveridge, and P. A. Dobosh, *J. Chem. Phys.* **47,** 2026 (1967).
38. N. S. Ostlund, *Quant. Chem. Prog. Exch. IX,* 224 (1972).

39. J. A. Pople and M. Gordon, *J. Am. Chem. Soc.* **89,** 4253 (1967).
40. C. Altona, J. H. Ippel, A. J. A. Westra Hoekzema, C. Erkelens, M. Groesbeek, and L. A. Donders, *Magn. Reson. Chem.* **27,** 564 (1989).
41. J. W. Coomber and E. Whittle, *J. Chem. Soc.,* 6661 (1965).
42. G. A. Olah and M. B. Comisarow, *J. Am. Chem. Soc.* **91,** 2955 (1969).
43. N. Muller and D. T. Carr, *J. Phys. Chem.* **67,** 112 (1963).
44. R. J. Abraham, M. Edgar, L. Griffiths, and R. L. Powell, *J. Chem. Soc. Perkin Trans.* **2,** 561 (1996).
45. A. Baklouti and J. Jullien, *Bull. Soc. Chim. France,* 2929 (1968).
46. E. L. Eliel and R. J. L. Martin, *J. Am. Chem. Soc.* **90,** 682 (1968).
47. J. B. Zhara, B. Waegell, and H. Bodot, *Bull. Soc. Chim. France,* 1107 (1974).
48. J. M. Bakke, L. H. Bjerkeseth, T. E. C. L. Ronnow, and K. Steinvoll, *J. Mol. Struct.* **321,** 205 (1994).
49. J. Adamson, A. B. Foster, L. D. Hall, R. N. Johnson, and R. H. Hesse, *Carbohydrate Res.* **15,** 351 (1970).
50. J. Adamson, A. B. Foster, L. D. Hall, and R. H. Hesse, *Chem. Commun.,* 309 (1969).
51. A. B. Foster, R. Hems, and L. D. Hall, *Can J. Chem.* **48,** 3937 (1970).
52. A. D. Barford, A. B. Foster, J. H. Westwood, and L. D. Hall, *Carbohydrate Res.* **11,** 287 (1969).
53. A. B. Foster, R. Hems, and J. H. Westwood, *Carbohydrate Res.* **15,** 41 (1970).
54. L. D. Hall and J. F. Manville, *Can J. Chem.* **47,** 361 (1969).
55. L. D. Hall and J. F. Manville, *Chem Commun.,* 47 (1968).
56. L. D. Hall, R. N. Johnson, A. B. Foster, and J. H. Westwood, *Can J. Chem.* **49,** 118 (1971).
57. L. D. Hall, R. N. Johnson, A. B. Foster, and J. H. Westwood, *Can J. Chem.* **49,** 236 (1971).
58. R. J. Abraham, H. D. Banks, E. L. Eliel, O. Hofer, and M. K. Kaloustian, *J. Am. Chem. Soc.* **94,** 1913 (1972).
59. A. D. Barford, A. B. Foster, J. H. Westwood, L. D. Hall, and R. N. Johnson, *Carbohydrate Res.* **19,** 49 (1971).
60. L. D. Hall and D. L. Jones, *Can. J. Chem.* **51,** 2925 (1973).
61. A. M. Ihrig and S. L. Smith, *J. Am. Chem. Soc.* **92,** 759 (1970).
62. J. L. Marshall, S. R. Walter, M. Barfield, A. P. Marchand, N. W. Marchand, and A. L. Segre, *Tetrahedron* **32,** 537 (1976).
63. S. Watanabe and I. Ando, *J. Mol. Struct.* **104,** 155 (1983).
64. N. L. Allinger, Y. H. Yuh, and J.-H. Lii, *J. Am. Chem. Soc.* **111,** 8551 (1989).
65. J. Guilleme, J. San Fabian, and E. Diez, *Mol. Phys.* **91,** 343 (1997).